Am J Transl Res 2018;10(9):2949-2957
www.ajtr.org /ISSN:1943-8141/AJTR0077047

Original Article

Gd-EOB-DTPA DCE-MRI biomarkers in a rabbit model of liver fibrosis

Yang Ji[1], Chuanshan Zhang[2], Zhe Huang[3], Xia Wang[3], Lina Yue[4], Meimei Gao[4], Huiling Hu[4], Qinjun Su[5], Yuedong Han[3,4], Bin Liu[5], Ding Yang[6], Zhanliang Su[7], Zhuoli Zhang[7]

[1]Department of Imaging Center, First Affiliated Hospital, Xi'an Medical University, Xi'an, Shaanxi, China; [2]Department of Pathology, Third Central Hospital, Tianjin, China; [3]Department of Radiology, Gaoxin Hospital, Xi'an Jiao Tong University, Xi'an, Shaanxi, China; [4]Department of Imaging Center, Lanzhou General Hospital of Lanzhou Military Area Command, Lanzhou, Gansu, China; [5]Department of Pathology, Lanzhou General Hospital of Lanzhou Military Area Command, Lanzhou, Gansu, China; [6]Department of Biomedical Engineering, University of Florida, Gainesville, FL, USA; [7]Department of Radiology, Feinberg School of Medicine, Northwestern University Chicago, IL, USA

Received March 30, 2018; Accepted June 15, 2018; Epub September 15, 2018; Published September 30, 2018

Abstract: The purpose of this study was to investigate the correlations between Gd-EOB-DTPA DCE-MRI biomarkers and histopathologic biomarkers of liver fibrosis progression in a rabbit model of liver fibrosis. Thirty-Six New Zealand white rabbits were randomly divided into control (n = 6) and liver fibrosis group (n = 30). Each rabbit in the liver fibrosis group received a weekly subcutaneous injection in the back comprising 50% carbon tetrachloride (CCl_4) in oily solution. Control rabbits received subcutaneous injections with the same amount of normal saline solution instead. MR imaging was performed in control and fibrotic rabbits were conducted by MRI at week 0 (n = 36). The fibrotic rabbits were performed MR imaging on 6 weeks, 9 weeks, and 12 weeks after modeling of fibrosis. Before each MRI, peripheral blood was collected, and several biochemical testes are performed. The thirty-four rabbits completed this study. They were then divided into three subgroups according to fibrotic stage: no fibrosis (F0, n = 12), mild fibrosis (F1+F2, n = 14), and advanced fibrosis (F3+F4, n = 8). DCE-MRI measurements show increasing K^{trans} and V_e while decreasing iACU90 with increasing fibrosis stage. The significant correlations were observed between mean K^{trans}, V_e, iACU90 and percentage of the animal with mild liver fibrosis. For blood biomarkers, there were significant differences between F0 and F1+F2, and between F0 and F3+F4 in the serum levels of ALT (all $P < 0.05$), and TB (F0 vs. F1+F2, $P = 0.004$), while no differences were found between F1+F2 group and F3+F4 group (all $P > 0.05$). There were significant differences between F0 and F1+F2 ($P = 0.02$). Gd-EOB-DTPA DCE-MRI is a promising method for the noninvasive diagnosis and staging of liver fibrosis. Future studies to evaluate the effectiveness of these techniques in patients with liver fibrosis are warranted.

Keywords: Liver fibrosis, animal, magnetic resonance imaging, pathology

Introduction

Advanced liver fibrosis can lead to cirrhosis, liver failure, portal hypertension, and liver cancer, which often requires liver transplantation as a life-saving procedure [1]. It is reversible in the early stages of liver fibrosis because the liver functions relatively well; therefore, early detecting of liver fibrosis is essential for treatment and prognosis [2]. Liver biopsy is the standard method for the diagnosis and staging of liver fibrosis. However, it is invasive, with associated pain and major complications reportedly occurring in 40.0% and 0.5% of patients, respectively [3]. Sampling errors can occur owing to the heterogeneous distribution of fibrosis in the liver and the relatively small biopsy samples [3]. Intra- and interobserver variations in histologic examinations can also lead to diagnosis error. Noninvasively quantitative imaging biomarkers would be particularly useful for serial evaluation of the effectiveness of liver fibrosis therapies [4].

Several magnetic resonance imaging (MRI) techniques have been used to assess liver fibro-

sis in preclinical and clinical settings, including MR elastography (MRE), diffusion-weighted imaging (DWI), Carbogen gas-challenge blood oxygen level-dependent (BOLD), and dynamic contrast-enhanced MRI (DCE-MRI) [4]. Meta-analysis studies show that MRE has high accuracy for the diagnosis of liver fibrosis and cirrhosis. Measurement of liver stiffness in MRE can be affected by several factors, including the cause of fibrosis, inflammation, hepatic metabolic and synthetic function, and technical limitations [5]. Compared with MRE, DWI has moderate accuracy for assessment of liver fibrosis, and calculation of the apparent diffusion coefficient can be affected by perfusion effects, liver inflammation, and liver steatosis [6]. Carbogen gas-challenge BOLD MR imaging can depict hepatic hemodynamic alterations during the progression of fibrosis [7]. However, it is difficult to co-register the MR images with the histologic specimens and because fibrosis would progress homogeneously in each animal's liver. DCE-MRI approaches have been used for assessment of liver fibrosis. Liver fibrosis assessment using pharmacokinetic parameters (imaging biomarkers), including the volume transfer constant (K^{trans}), the flux rate constant (k_{ep}), the volumefraction V_e of the extravascular extracellular space (EES), and the plasma volume fraction (v_p) [8].

In this study, gadolinium ethoxybenzyl diethylenetriaminepentaacetic acid (Gd-EOB-DTPA), a newly developed MR contrast agent, was used. Gd-EOB-DTPA is an ionic complex consisting of gadolinium (III) and the ligand ethoxybenzyl-diethylenetriaminepentaacetic acid (EOB-DTPA). The purpose of our study was to investigate the correlations between Gd-EOB-DTPA DCE-MRI biomarkers and histopathologic biomarkers of liver fibrosis progression in a rabbit model of liver fibrosis.

Materials and methods

All studies were approved by our institutional animal care and use committee and were performed in accordance with the NIH guidelines.

Animal model and experimental design

Thirty-six male/female healthy New Zealand white rabbits (5 months age from Experimental Animal Center of Lanzhou University) that initially weighted 1.8-2.7 kg were used for this study. The rabbits were randomly divided into control (n = 6) and liver fibrosis group (n = 30). Each rabbit in the liver fibrosis group received a weekly subcutaneous injection in the back comprising 50% carbon tetrachloride (CCl_4) in oily solution (ratio 1:1) (0.2 ml/kg) [9]. Control rabbits received subcutaneous injections with the same amount of normal saline solution instead.

MR imaging was performed in control and fibrotic rabbits were conducted by MRI at week 0 (n = 36). The fibrotic rabbits were performed MR imaging on 6 weeks, 9 weeks, and 12 weeks after modeling of fibrosis (each n = 10).

Blood tests for assessment of liver function

The peripheral blood (3-5 ml) was collected via the ear border vein after modeling of fibrosis at 0, 6, 9, and 12 weeks (control rabbit at week 0). Blood samples were sent to the core facilities and several biochemical testes are performed including alanine aminotransferase (ALT), aspartate transaminase (AST), and total bilirubin (TB) levels. The levels of serum hyaluronic acid (HA), collagen type IV (IV-C), and procollagen type III (PC III) were also measured.

MRI examinations

All MRI examinations were performed by using a 3.0-T clinical MR unit (Verio 3.0T, Siemens Medical Solutions, Erlangen, Germany) with a 32-channel head phased-array coil (Siemens Medical Solutions, Erlangen, Germany). Before being imaged, rabbits were anesthetized with intramuscular administration of 0.3 mL per kilogram of body weight of 2% xylazine hydrochloride and 30 mg/kg of ketamine hydrochloride. Additional xylazine hydrochloride was given intravenously as required. Animals were fixed on rabbit holder. Following acquisition of coronal and transverse turbo spin-echo (TSE) T1-weighted (T1W) and T2W anatomical images, transverse T1 mapping and T2 mapping were obtained with fat suppression. For Gd-EOB-DTPA DCE-MRI, administration of Gd-EOB-DTPA was done as a bolus with a total 0.025 mmol/kg and injection within 3 s through the ear vein, followed by 2 ml saline chaser at the same rate. For all animals, T1W volumetric interpolated breath-hold examination (VIBE) was performed for T1W from pre-contrast 2 mins topost-contrast 20 mins. The MRI parameters were shown in **Table 1**.

Table 1. MRI pulse sequences and common scan parameters

Purpose	Sequences	Scan parameters
Anatomic imaging	T2W TSE	TR/TE = 4000/30 ms, TF = 15, FOV = 210 × 210 mm, matrix = 256 × 256, ST = 4 mm
T1 mapping	Variableflip angle	TR/TE = 15/2 ms, FA = 5°/26°, FOV = 210 × 210 mm, matrix = 320 × 320, ST = 4 mm, ST = 2:15 mins
T2 mapping	Multi-echo SE	TR/TE = 2000/10, 21, 31, 42, 52, 63 ms, FA = 180°, FOV = 210 × 210 mm, matrix = 320 × 320, ST = 4 mm, scan time = 2:52 mins
DCE-MRI	VIBE	TR/TE = 4.8/1.4 ms, FA = 5°/15°, FOV = 101 × 140 mm, matrix = 59 × 128, ST = 2 mm, scan time = 2:52 mins

T2W: T2-weighted; TSE: turbo spin-echo; TR: repetition time; TE: echo time; ST: slice thickness; FA: flip angle; FOV: Field of view; ST: scan time; TF: turbo-factor; VIBE: volumetric interpolated breath-hold examination; DCE-MRI: dynamic contrast-enhanced MRI.

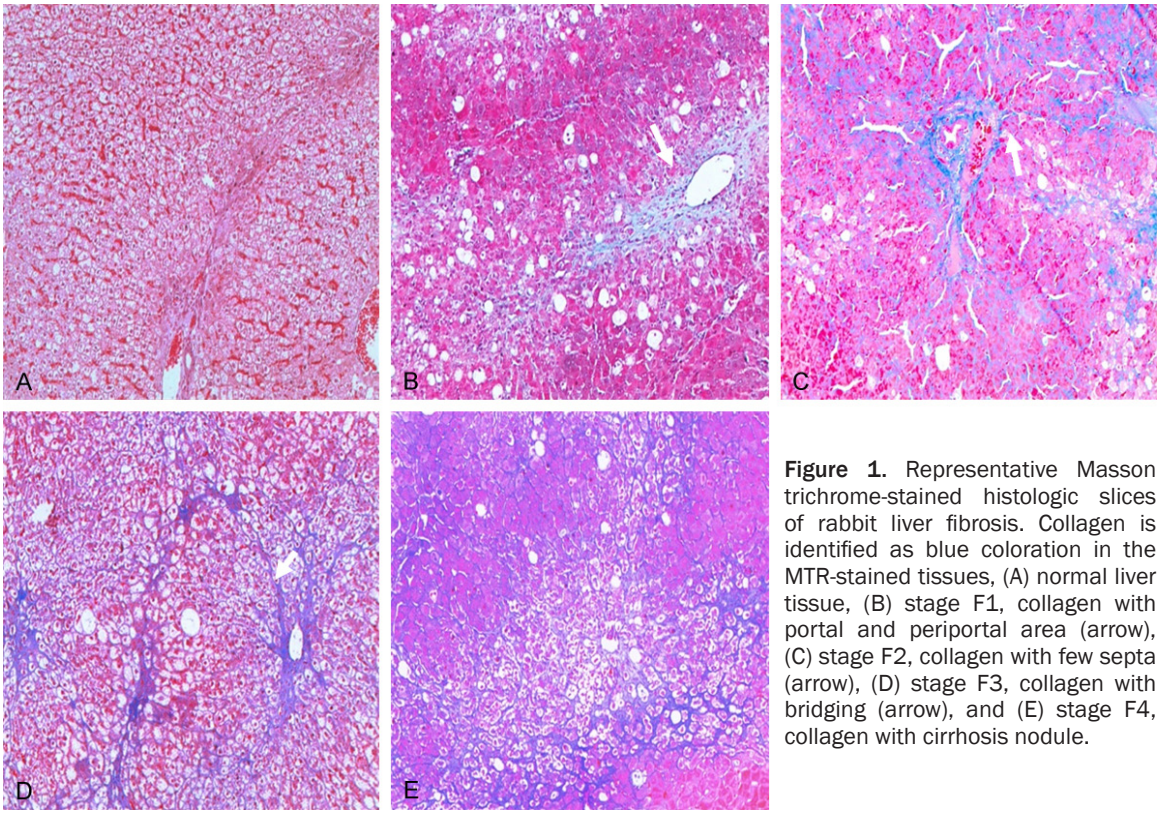

Figure 1. Representative Masson trichrome-stained histologic slices of rabbit liver fibrosis. Collagen is identified as blue coloration in the MTR-stained tissues, (A) normal liver tissue, (B) stage F1, collagen with portal and periportal area (arrow), (C) stage F2, collagen with few septa (arrow), (D) stage F3, collagen with bridging (arrow), and (E) stage F4, collagen with cirrhosis nodule.

Histologic evaluation

After modeling of fibrosis at 6 weeks, 9 weeks, and 12 weeks, each rabbit was euthanized with an i.v. administration of 150 to 200 mg/kg sodium pentobarbital (Euthasol, Delmarva Laboratories, Midlothian, VA) 3 hours after MR examinations. Three histologic slices excised from the left lateral, right lateral, and medium lateral liver lobes of each rabbit were fixed in 10% buffered formaldehyde solution, embedded in paraffin, and sliced (4 μm slice thickness). The slides were submitted to the pathology core facility for Masson's trichrome staining which was used to identify collagen tissue. A pathologist who specializes in gastrointestinal oncology (L.W., > 10 years' experience) first assessed the stage of liver fibrosis according to the METAVIR scoring system: Stage F0 indicates no fibrosis; stage F1, portal fibrosis without septa; stage F2, portal fibrosis with few septa; stage F3, numerous septa without cirrhosis; and F4, cirrhosis. These slides (4 slices/each animal) were scanned at 200 × magnifica-

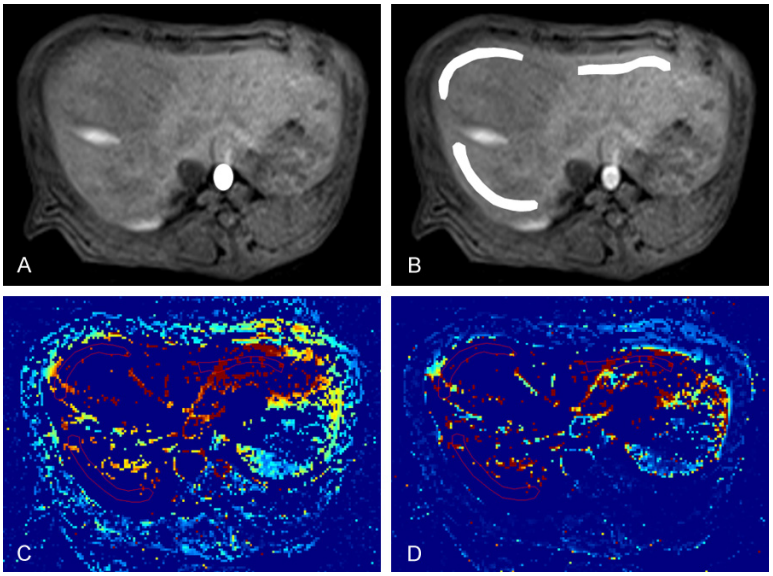

Figure 2. DCE-MRI measurements of the rabbit liver. The arterial input function (AIF) was measured at abdominal aorta (A). Three ROIs were drawn by hand in the left lateral, right lateral, and medium lateral liver lobes to measure mean values (B). Each ROI was avoided large vessels. Pharmacokinetic parametric maps for K^{trans} (C) and V_e (D).

tionanddigitizedusingTissueFAXSsystem(TissueGnostics, Vienna, Austria). Collagen fibers were stained aniline blue, while hepatocytes were stained red (**Figure 1**). The fibrotic region was identified by extracting the area of blue components with use of offline ImageJ postprocessing software (National Institutes of Health, Bethesda, MD, USA). Fibrotic deposition was expressed as the ratio of stained collagen tissue area to total area measured in the analyzed field.

Image analysis

Image analysis was performed by two radiologists in consensus (H.Y. with 10 years of experience in abdominal MR imaging, and, S.Z. with 5 years of experience). Both radiologists were blinded to the histopathologic results. Quantitative parameters including K^{trans}, V_e, and area under the contrast concentration versus time curve 90 seconds after contrast injection (IAUC90) of the liver parenchyma were estimated from DCE-MRI data at an image processing workstation (Syngo MMWP, Siemens Medical Solutions). The arterial input function (AIF) was measured at abdominal aorta and the venous input function (VIF) was measured at the main portal vein. Three circular regions of interest (ROI) were drawn by hand in the left lateral, medium lateral, right lateral liver lobes to measure mean values. Each ROI was avoided large vessels and pharmacokinetic parametric maps were generated by DCE-MRI data (**Figure 2**).

Statistical analyses

The animals were grouped into three: no fibrosis (F0), mild fibrosis (F1 and F2), and advanced fibrosis (F3 and F4) [10]. Data were expressed as mean ± standard deviation (SD). Data were first tested for normality by using a one-sample Kolmogorov-Smirnov test. DCE-MRI imaging and blood biomarkers were compared between the three groups at analysis of variance and then at two-by-two comparisons performed with independent-sample *t* testing. The relationships between percentage of histological liver fibrosis and changes of DCE-MRI biomarkers were assessed by calculating Spearman correlation coefficients. Statistical analysis results were significant at $P < 0.05$. All statistical analyses were performed by using SPSS software (SPSS, Chicago, Ill).

Results

Of the thirty-six rabbits, two rabbits in the liver fibrosis group died during the experiment. A total of thirty-four rabbits completed the study, with twelve of those at stage F0 (control group). In the liver fibrosis group, eight rabbits were stage F1, six were stage F2, five were stage F3, and three were stage F4 (**Figure 2**). The thirty-four rabbits were then divided into three subgroups according to fibrotic stage: no fibrosis (F0, n = 12), mild fibrosis (F1+F2, n = 14), and advanced fibrosis (F3+F4, n = 8).

Blood biomarkers were shown in **Figure 3**. There were significant differences between F0 and F1+F2, and between F0 and F3+F4 in the serum levels of ALT (F0 vs. F1+F2, $P < 0.001$; F0 vs. F3+F4, $P = 0.001$), AST (F0 vs. F1+F2, $P < 0.001$; F0 vs. F3+F4, $P = 0.001$), and TB (F0 vs. F1+F2, $P = 0.004$), while no differences

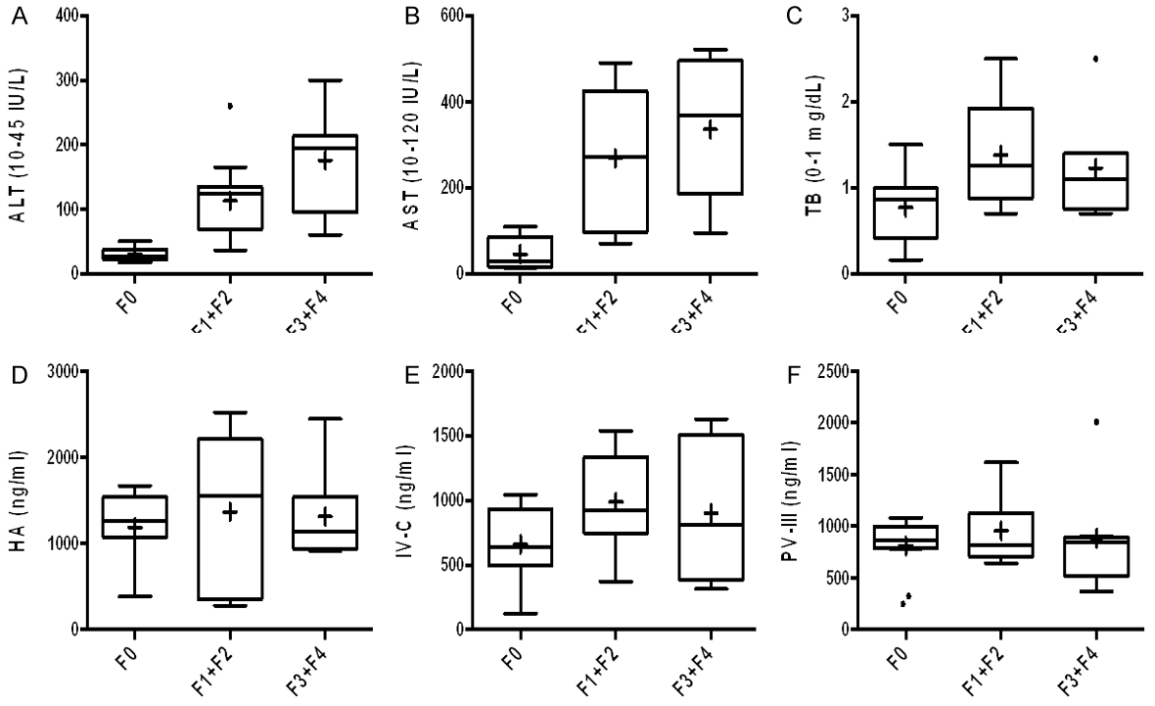

Figure 3. Rabbit liver function assessment by blood biomarkers. There were significant differences in the serum levels of ALT between F0 and F1+F2, and between F0 and F3+F4 (F0 vs. F1+F2, P < 0.001; F0 vs. F3+F4, P = 0.001) (A), in the serum levels of AST (F0 vs. F1+F2, P < 0.001; F0 vs. F3+F4, P = 0.001) (B), and TB (F0 vs. F1+F2, P = 0.004) (C), while no differences in both the serum levels of ALT and AST between F1+F2 group and F3+F4 group (all P > 0.05). No significant differences were found between F0 and F3+F4 in the serum levels of TB (P = 0.08). There were no significant differences in HA levels at the different groups (all P > 0.05) (D). There were significant differences between F0 and F1+F2 (P = 0.02), while no differences were found in IV-C levels between F0 and F1+F2, and between F1+F2 and F3+F4 (all P > 0.05) (E). There were no significant differences in PC III level at the different groups (all P > 0.05) (F).

Table 2. The serum biomarkers measurements

Serum markers	No fibrosis (F0, n = 12)	Mild fibrosis (F1+F2, n = 14)	Advanced fibrosis (F3+F4, n = 8)
ALT (IU/L)	30.08 ± 10.56	113 ± 57.56	175.75 ± 73.31
AST (IU/L)	45.25 ± 32.49	268.07 ± 154.03	335.5 ± 150.07
BT (mg/dl)	0.77 ± 0.38	1.38 ± 0.56	1.27 ± 0.55
HA (ng/ml)	1188.67 ± 408.21	1365.57 ± 833.46	1314.25 ± 484.83
IV-C (ng/ml)	661.5 ± 263.45	987.64 ± 337.80	902.75 ± 510.69
PC III (ng/ml)	810.08 ± 252.26	957.36 ± 328.02	886.38 ± 468.34

ALT: aminotransferase; AST: aspartate transaminase; TB: total bilirubin; HA: hyaluronic acid; IV-C; collagen type IV; PC III: procollagen type III.

were found between F1+F2 group and F3+F4 group (all P > 0.05) (**Table 2**). No significant difference was found between F0 and F3+F4 in TB (P = 0.08). No significant differences were founded in HA levels at the different groups (all P > 0.05). There were significant differences between F0 and F1+F2 (P = 0.02), while no differences were found in IV-C levels between F0 and F1+F2, and between F1+F2 and F3+F4 (all P > 0.05). There are no significant differences in PC III level at the different groups (all P > 0.05).

DCE-MRI measurements show increasing K^{trans} and V_e while decreasing iACU90 with increasing fibrosis stage (**Figure 4**). In **Figure 4A**, representative transverse anatomic MR images (T1W and T2W), K^{trans}, and V_e maps from no fibrosis group (stage F0, upper row) and advanced fibrosis (stage F3, lower row) animals. **Figure 4B** shows K^{trans}, V_e, and iACU90 measurements in no fibrosis group (F0 stage), mild fibrosis group (F1+F2 stages), and advanced fibrosis group (F3+F4 stages). The significant correlations were observed between mean K^{trans}, V_e, iACU90 and percentage of the animal with mild liver fibrosis (**Figure 4C**).

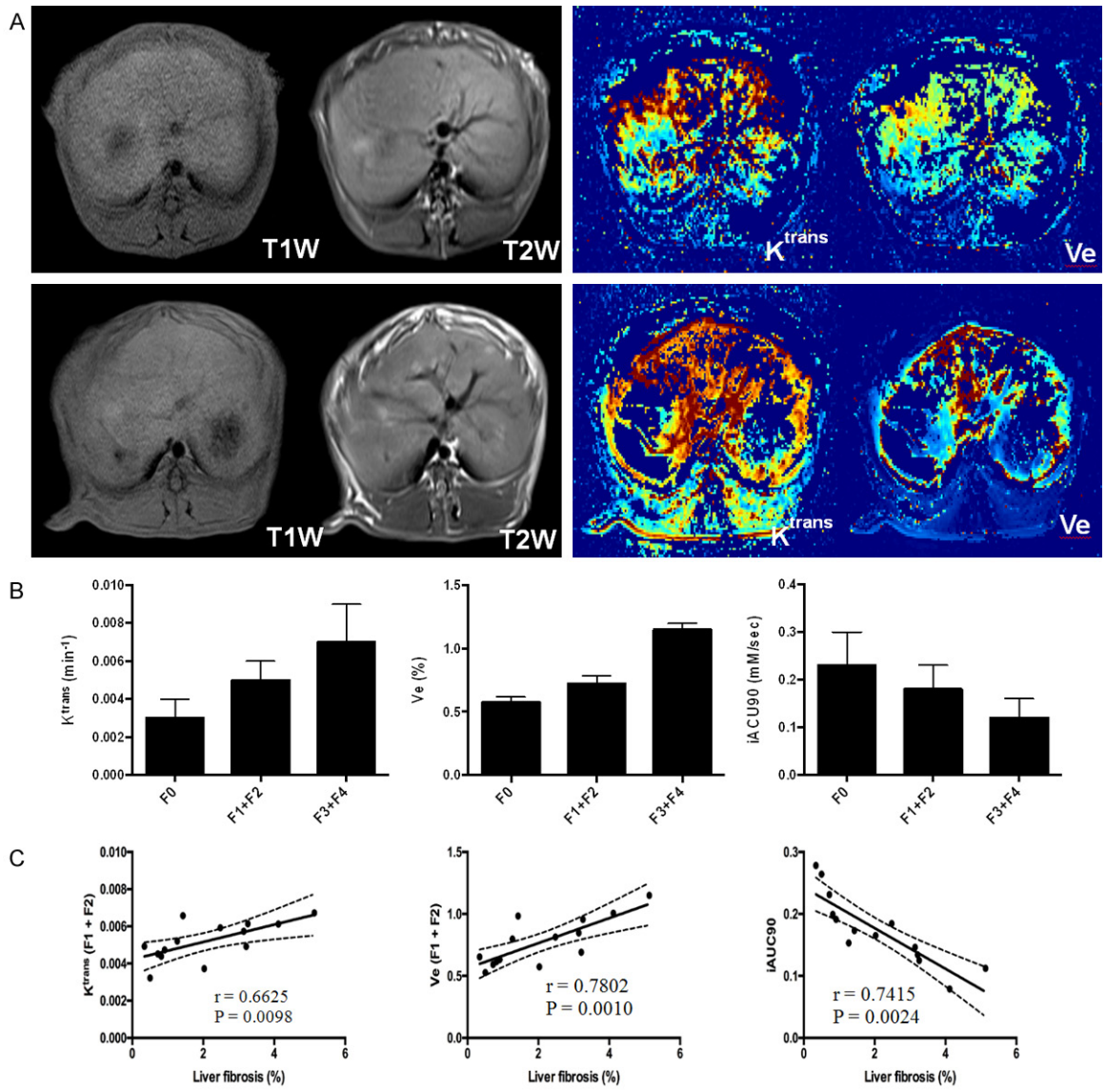

Figure 4. Liver fibrosis assessment by DCE-MRI measurements. A. Representative transverse anatomic MR images (T1W and T2W), K^{trans} and Ve maps from no fibrosis group (stage F0, upper row) and advanced fibrosis (stage F3, lower row) animals. B. Quantitative measurements, there were significant differences mean K^{trans} between advanced fibrosis group and no fibrosis group (P = 0.03), between advanced fibrosis group and mild fibrotic group (P = 0.01), and between no fibrosis group and mild fibrosis group (P = 0.024). There were significant differences in mean Ve between no fibrosis and advanced fibrosis (P = 0.015), between mild fibrosis and advanced fibrosis (0.032), but no significant difference between no fibrosis and mild fibrosis (P = 0.18). The significant differences were founded in mean iACU90 between no fibrosis and advanced fibrosis (P = 0.021), between mild fibrosis and advanced fibrosis (P = 0.045), and between no fibrosis and mild fibrosis (P = 0.023). C. The significant correlations were observed between mean K^{trans}, V_e, iACU90 and percentage of the animal with mild liver fibrosis.

Discussion

We have shown that non-invasive Gd-EOB-DTPA DCE-MRI radiologic or serum-based markers are considered categorical parameters of liver fibrosis. There were significant differences between F0 and F1+F2 (P = 0.02) in IV-C levels, while no differences were found between F0 and F1+F2, and between F1+F2 and F3+F4 (all P > 0.05). DCE-MRI measurements show increasing K^{trans}, V_e, and decreasing iACU90 with increasing fibrotic stage. The significant correlations were observed between mean K^{trans}, V_e, iACU90 and percentage of the animal with mild liver fibrosis.

The model used in this study has been demonstrated that cellular alterations and histologic

patterns are similar to those in human liver fibrosis [9, 11]. However, having considerable individual variation in the speed of fibrosis progression, leads a variable number of rabbits had each stage of fibrosis [9, 11]. Hence, we did not evaluate changes between the acute and chronic stages of liver fibrosis. Future studies to examine the relationship between these functional measurements at the acute and chronic stages are warranted. Due to the extensive individual variation of liver fibrotic progression, we could not compare the DCE-MRI measurements of responses between the five METAVIR stages [12, 13]. However, the significant differences were observed between the animals in each of the three clinically relevant fibrosis groups (no substantial fibrosis, stage F0), mild fibrosis (F1+F2), and advanced fibrosis (F3+F4).

Liver biopsy is considered as the gold standard for diagnosis of and staging of liver fibrosis [14]. However, liver biopsy is an invasive and inaccurate gold standard with numerous drawbacks [14, 15]. To overcome the limitations of liver biopsy, several non-invasive techniques have been investigated for the assessment of liver fibrosis [13, 16]. Non-invasive biomarkers of liver fibrosis can be radiologic [17] or serum-based [18]. Radiologic techniques based on ultrasound, MRI, and elastography have been used to assess liver fibrosis [17]. Serum-based biomarkers of liver fibrosis have also been developed [18, 19]. These are broadly classified into indirect and direct biomarkers. Indirect biomarkers reflect liver function. Direct biomarkers reflect extracellular matrix turnover, and include molecules involved in hepatic fibrogenesis. This study includes both radiologic and serum biomarkers show that both biomarkers of liver fibrosis correlate with histological results. This feature is certainly clinically useful [20].

In previous Gd-EOB-DTPA DCE-MRI studies involving the evaluation of rat and rabbit liver fibrosis [21, 22]. In this study, fibrotic deposition was quantitively measured and the significant correlations were observed between mean K^{trans}, V_e, iACU90 and percentage of the animal with mild liver fibrosis, which is early stage of liver fibrosis. Therefore, this study results provide strong evidence of the immediate feasibility of clinical translation because we used a 3.0-T clinical MR unit and standard DCE-MRI sequences that are available on most clinical MR systems. Using serum-based biomarkers to assess liver fibrosis, current studies showed a 50% sensitivity and 61% specificity [23].

There were several limitations to our current study. First, we measured the means of imaging biomarkers for the entire liver rather than for specific liver regions on each image section because it was difficult to co-register the MR images with the histologic specimens. In this case, we assumed a priori that liver fibrosis would progress homogeneously in each animal's liver. However, variations in imaging biomarkers and liver activation were observed and probably resulted from the differing blood supply in the different liver regions and/or the different levels of fibrosis. Future studies to further investigate these intrahepatic differences in DCE-MRI response in specific regions or lobes in the liver should be performed. Furthermore, we performed MRI studies in each animal at a single time point, not serially follow up each animal because of the logistic complexities involved in serially following up the animals during these processes and our desire for reference-standard histologic confirmation of the fibrosis stages, which required that each animal is sacrificed to harvest their livers. In future studies, fibrosis progression could be followed in each animal.

In conclusion, Gd-EOB-DTPA DCE-MRI is a promising method for the noninvasive diagnosis and staging of liver fibrosis Future studies to evaluate the effectiveness of these techniques in patients with liver fibrosis are warranted.

Acknowledgements

This work was supported by natural science foundation research project by Shaanxi province (No: S2015YFJM1473) and grants R01CA-196967 and R01CA209886 funded by the USA National Cancer Institute (National Institutes of Health).

Disclosure of conflict of interest

None.

Address correspondence to: Yuedong Han, Department of Radiology, Gaoxin Hospital, Xi'an Jiao Tong University, No.16, South Tuanjie Road, Xi'an, Shaan-

xi, China. Tel: (086-029) 88330016; Fax: (086-029) 88330066; E-mail: hanyuedong@126.com; Bin Liu, Department of Pathology, Lanzhou General Hospital of Lanzhou Military Area Command, No.333, South Binhe Road, Qilihe District, Lanzhou, Gansu, China. Tel: (086-0931) 8994567; Fax: (086-0931) 8994-597; E-mail: liumb@189.cn

References

[1] Perumpail BJ, Khan MA, Yoo ER, Cholankeril G, Kim D and Ahmed A. Clinical epidemiology and disease burden of nonalcoholic fatty liver disease. World J Gastroenterol 2017; 23: 8263-8276.

[2] Xiao H, Shi M, Xie Y and Chi X. Comparison of diagnostic accuracy of magnetic resonance elastography and fibroscan for detecting liver fibrosis in chronic hepatitis B patients: a systematic review and meta-analysis. PLoS One 2017; 12: e0186660.

[3] Parikh ND, Singal AG and Hutton DW. Cost effectiveness of regorafenib as second-line therapy for patients with advanced hepatocellular carcinoma. Cancer 2017; 123: 3725-3731.

[4] Horowitz JM, Venkatesh SK, Ehman RL, Jhaveri K, Kamath P, Ohliger MA, Samir AE, Silva AC, Taouli B, Torbenson MS, Wells ML, Yeh B and Miller FH. Evaluation of hepatic fibrosis: a review from the society of abdominal radiology disease focus panel. Abdom Radiol (NY) 2017; 42: 2037-2053.

[5] Xiao G, Zhu S, Xiao X, Yan L, Yang J and Wu G. Comparison of laboratory tests, ultrasound, or magnetic resonance elastography to detect fibrosis in patients with nonalcoholic fatty liver disease: a meta-analysis. Hepatology 2017; 66: 1486-1501.

[6] Tan CH and Venkatesh SK. Magnetic resonance elastography and other magnetic resonance imaging techniques in chronic liver disease: current status and future directions. Gut Liver 2016; 10: 672-686.

[7] Zhang LJ, Zhang Z, Xu J, Jin N, Luo S, Larson AC and Lu GM. Carbogen gas-challenge blood oxygen level-dependent magnetic resonance imaging in hepatocellular carcinoma: initial results. Oncol Lett 2015; 10: 2009-2014.

[8] Aronhime S, Calcagno C, Jajamovich GH, Dyvorne HA, Robson P, Dieterich D, Fiel MI, Martel-Laferriere V, Chatterji M, Rusinek H and Taouli B. DCE-MRI of the liver: effect of linear and nonlinear conversions on hepatic perfusion quantification and reproducibility. J Magn Reson Imaging 2014; 40: 90-98.

[9] Zou L, Jiang J, Zhong W, Wang C, Xing W and Zhang Z. Magnetic resonance elastography in a rabbit model of liver fibrosis: a 3-T longitudinal validation for clinical translation. Am J Transl Res 2016; 8: 4922-4931.

[10] Kim HS, Rotundo L, Kothari N, Kim SH and Pyrsopoulos N. Vitamin D is associated with severity and mortality of non-alcoholic fatty liver disease: a US population-based study. J Clin Transl Hepatol 2017; 5: 185-192.

[11] Wang MJ, Ling WW, Wang H, Meng LW, Cai H and Peng B. Non-invasive evaluation of liver stiffness after splenectomy in rabbits with CCl4-induced liver fibrosis. World J Gastroenterol 2016; 22: 10166-10179.

[12] Carrasco I, Arias A, Benitez-Gutierrez L, Lledo G, Requena S, Cuesta M, Cuervas-Mons V and de Mendoza C. Baseline NS5A resistance associated substitutions may impair DAA response in real-world hepatitis C patients. J Med Virol 2018; 90: 532-536.

[13] Pokorska-Spiewak M, Kowalik-Mikolajewska B, Aniszewska M, Pluta M and Marczynska M. Clinical usefulness of new noninvasive serum biomarkers for the assessment of liver fibrosis and steatosis in children with chronic hepatitis C. Clin Exp Hepatol 2017; 3: 198-202.

[14] Lambrecht J, Verhulst S, Mannaerts I, Reynaert H and van Grunsven LA. Prospects in non-invasive assessment of liver fibrosis: liquid biopsy as the future gold standard? Biochim Biophys Acta 2018; 1864: 1024-1036.

[15] Dhingra S, Ward SC and Thung SN. Liver pathology of hepatitis C, beyond grading and staging of the disease. World J Gastroenterol 2016; 22: 1357-1366.

[16] Valva P, Rios D, Casciato P, Gadano A, Galdame O, Mullen E, Bertot G, de Matteo E and Preciado MV. Nonalcoholic fatty liver disease: biomarkers as diagnostic tools for liver damage assessment in adult patients from Argentina. Eur J Gastroenterol Hepatol 2018; 30: 637-644.

[17] Younossi ZM, Loomba R, Anstee QM, Rinella ME, Bugianesi E, Marchesini G, Neuschwander-Tetri BA, Serfaty L, Negro F, Caldwell SH, Ratziu V, Corey KE, Friedman SL, Abdelmalek MF, Harrison SA, Sanyal AJ, Lavine JE, Mathurin P, Charlton MR, Goodman ZD, Chalasani NP, Kowdley KV, George J and Lindor K. Diagnostic modalities for non-alcoholic fatty liver disease (NAFLD), non-alcoholic steatohepatitis (NASH) and associated fibrosis. Hepatology 2018; 68: 349-360.

[18] Pateu E, Oberti F and Cales P. The noninvasive diagnosis of esophageal varices and its application in clinical practice. Clin Res Hepatol Gastroenterol 2018; 42: 6-16.

[19] Shirabe K, Bekki Y, Gantumur D, Araki K, Ishii N, Kuno A, Narimatsu H and Mizokami M. Mac-2 binding protein glycan isomer (M2BPGi) is a new serum biomarker for assessing liver fibro-

sis: more than a biomarker of liver fibrosis. J Gastroenterol 2018; 53: 819-826.
[20] Nallagangula KS, Nagaraj SK, Venkataswamy L and Chandrappa M. Liver fibrosis: a compilation on the biomarkers status and their significance during disease progression. Future Sci OA 2018; 4: Fso250.
[21] Giraudeau C, Leporq B, Doblas S, Lagadec M, Pastor CM, Daire JL and Van Beers BE. Gadoxetate-enhanced MR imaging and compartmental modelling to assess hepatocyte bidirectional transport function in rats with advanced liver fibrosis. Eur Radiol 2017; 27: 1804-1811.
[22] Xie Y, Zhang H, Jin C, Wang X, Wang X, Chen J and Xu Y. Gd-EOB-DTPA-enhanced T1rho imaging vs. diffusion metrics for assessment liver inflammation and early stage fibrosis of nonalcoholic steatohepatitis in rabbits. Magn Reson Imaging 2017; 48: 34-41.
[23] Verma S, Jensen D, Hart J and Mohanty SR. Predictive value of ALT levels for non-alcoholic steatohepatitis (NASH) and advanced fibrosis in non-alcoholic fatty liver disease (NAFLD). Liver Int 2013; 33: 1398-1405.